Highlighting joint research results from Department of Chemical and Biomolecular Engineering, Korea Advanced Instituted Science and Technology (KAIST), and Department of Chemical and Biomolecular Engineering, Yonsei University, Korea.

Title: Facile preparation of water soluble CuPt nanorods with controlled aspect ratio and study on their catalytic properties in water

CuPt nanorods with various aspect ratios were synthesized and surface-modified by thiol terminated PEO chains to impart water solubility. Their catalytic properties in the aqueous phase were investigated using a reaction of OPD oxidation, demonstrating the excellent dispersion of nanorods in an aqueous solution. The effect of the aspect ratio on the catalytic properties of nanorods was also studied.

As featured in:

Journal of
Materials Chemistry
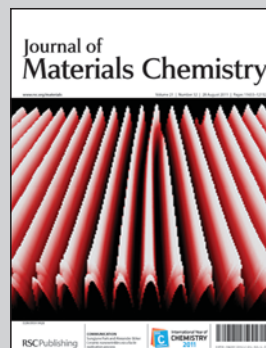
See Taegyun Kwon, Minkyu Min, Hyunjoo Lee and Bumjoon J. Kim
J. Mater. Chem., 2011, **21,** 11956.

RSCPublishing

www.rsc.org/materials

Dynamic Article Links ▶

PAPER

Facile preparation of water soluble CuPt nanorods with controlled aspect ratio and study on their catalytic properties in water†

Taegyun Kwon,[a] Minkyu Min,[b] Hyunjoo Lee[b] and Bumjoon J. Kim*[a]

CuPt nanorods, originally nonpolar, were modified by ligand exchange to become soluble in water. Three different CuPt nanorods with aspect ratios (ARs) of 1, 6, and 11 were produced with high monodispersity by a thermal decomposition method and a subsequent purification process. The synthesized nanorods were initially dispersed in nonpolar solvents such as hexane. Thiol-terminated poly(ethyleneoxide) (PEO-SH) was synthesized and attached to the surface of CuPt nanorods to impart water solubility. The nanorods were completely transferred to the aqueous phase. Their catalytic properties in the aqueous phase were investigated using a peroxidase-like reaction of *o*-phenylenediamine (OPD) oxidation. CuPt nanorods showed high activity for the reaction, demonstrating the excellent dispersion of nanorods in an aqueous solution. The effect of AR on the catalytic properties of nanorods was also studied.

Introduction

Metal nanoparticles have attracted a great deal of attention due to their potential in various applications such as electronic devices,[1,2] magnetic storage,[3] optical devices,[4–7] surfactants[8–10] and catalysis.[11–14] For these applications, precise control of both particle size and shape is critically important, since the properties of nanoparticles are strongly dependent on their size and shape.[15] In addition, because their separation is extremely difficult, synthetic methods that can produce nanoparticles with a uniform distribution of size and shape are highly desirable.

Metal nanoparticles can be synthesized by several methods, including photoreduction,[16–18] radiolytic reduction,[19,20] alcohol reduction[21] and polymer/surfactant reduction.[22,23] Of particular interest is the thermal decomposition method that can produce nanoparticles with excellent control over the size and uniformity, and in a relatively larger quantity.[24] This method requires nonpolar organic materials such as oleic acid or oleylamine as surface-stabilizing agents, which stabilize nanoparticles and prevent their aggregations. However, at the same time, such surface stabilizers on the nanoparticle behave as an insulating barrier and hinder access of other molecules to the surface of the particle, which is detrimental for catalytic applications. In addition, many applications—particularly in biological systems—require nanoparticles to be fully dispersed in a hydrophilic solvent or water without degradation of their properties. To overcome these problems, the surface modification of the as-synthesized nanoparticles is required to control their polarity, typically by replacing the original nonpolar stabilizers with the polar ones *via* a ligand-exchange process.[25–31] For example, hydrophilic polyvinyl pyrrolidone (PVP) has been widely used to replace the organic stabilizers on the particles and disperse them in polar solvents.[32,33] The ligand exchange procedure requires that PVP should have stronger binding to the nanoparticle surface than the original organic ligands. However, PVP molecules have a relatively weak C=O binding group compared to oleylamine.[32] Furthermore, PVP has long chain, which kinetically hinders the replacement of the oleylamine and oleic acid ligands on the nanoparticle *via* ligand exchange.[34] Therefore, it is difficult to achieve phase transfer of nanoparticles and ensure their stability in polar or aqueous media *via* ligand exchange with these molecules.

Herein, we report a simple route for producing water-soluble nanoparticles using thiol end-functionalized polymer ligands. First, we synthesized water-soluble and biocompatible poly(ethyleneoxide) (PEO) with a thiol end-group *via* a three-step reaction. It is well-known that the thiol group has a much stronger affinity to many metal surfaces including Au, Ag, Pt, *etc.* than oleylamine and oleic acid.[35–38] To show the versatility of our approach, we have applied thiol-terminated PEO chains (PEO-SH) to coat CuPt nanorods with various aspect ratios in the range of 1 to 11, which were originally dispersible only in nonpolar solvents such as hexane. The aspect ratios were carefully controlled by tuning the ratio between oleic acid and oleylamine. After ligand exchange, the nanorods were completely transferred to the aqueous phase. To demonstrate excellent

[a]Department of Chemical and Biomolecular Engineering, Korea Advanced Instituted Science and Technology (KAIST), Daejeon, 305-701, Korea. E-mail: bumjoonkim@kaist.ac.kr; Fax: +82-42-350-3910; Tel: +82-42-350-3935
[b]Department of Chemical and Biomolecular Engineering, Yonsei University, Seoul, 120-749, South Korea
† Electronic supplementary information (ESI) available. See DOI: 10.1039/c1jm11318f

This journal is © The Royal Society of Chemistry 2011

dispersion, and stability of nanorods in water, their catalytic properties in the aqueous phase were investigated using a peroxidase-like reaction of *o*-phenylenediamine (OPD) oxidation. In addition, the effect of aspect ratio on the catalytic performance was also carefully investigated. It was found that the spherical CuPt particles with aspect ratio (AR) of 1.0 showed the highest catalytic activity, while the longer CuPt nanorods (AR = 5.6 and 11.1) had lower activity, showing that the reactivity of nanorods was proportional to the amount of platinum atoms on the surface. These results clearly demonstrated that PEO functionalized CuPt nanorods not only were dispersed in water, but also retained a high catalytic activity in water.

Experimental section

Materials

Copper acetylacetonate (Cu(acac)$_2$, Sigma-Aldrich), platinum acetylacetonate (Pt(acac)$_2$, Sigma-Aldrich), 1,2-hexadecanediol (Sigma-Aldrich), oleic acid (OA, Sigma-Aldrich), oleylamine (OLA, Sigma-Aldrich), 1-octadecene (Sigma-Aldrich), poly(ethyleneoxide) (PEO-OH) (molecular weight (M_n) = 2.4 kg mol^{-1}, polydispersity index (PDI) = 1.05, Polymer Source), triethylamine (Sigma-Aldrich), dichloromethane (DCM, anhydrous, Sigma-Aldrich), methanesulfonyl chloride (Sigma-Aldrich), MgSO$_4$ (Sigma-Aldrich), tetrahydrofuran (THF, anhydrous, Junsei), potassium thioacetate (Sigma-Aldrich), concentrated HCl, chloroform, hydrogen peroxide (H$_2$O$_2$) and *o*-phenylenediamine (OPD, Sigma-Aldrich) were used as received.

Synthesis of CuPt nanorods with various aspect ratios

CuPt nanorods were synthesized by the thermal degradation method with the standard air free technique.[39] Typically, 24 mg Cu(acac)$_2$ and 43 mg Pt(acac)$_2$ were dissolved in 5 ml 1-octadecene. OA and OLA as capping agents (1.5 ml OA for spherical nanoparticles, 0.6 ml OLA and 0.8 ml OA for short nanorods, 0.8 ml OLA and 1.2 ml OA for long nanorods) and 1,2-hexadecanediol as the reducing agent (105 mg) were added to the reaction mixture. The solution was heated and stirred at 120 °C under a nitrogen atmosphere for 20 min to melt the precursors. The temperature was then increased to 225 °C and maintained for 30 min to prepare the product. The solution was cooled down to room temperature, and the product was precipitated in ethanol by centrifugation at 3600 rpm for 10 min. This sequence of steps afforded a precipitate that could be dispersed in hexane, cyclohexane and toluene.

Ligand exchange to form PEO-coated CuPt nanoparticles

First, PEO-SH was prepared *via* a three-step reaction by following a modified procedure from the literature[40] (Scheme S1†). As-prepared CuPt nanoparticles and PEO-SH (9 mg and 27 mg for spherical nanoparticles, 15 mg and 24 mg for short NRs, 13 mg and 19 mg for long NRs, respectively), which was equimolar with oleic acid and oleylamine ligands, were mixed with anhydrous THF (10 ml) at 40 °C for 6 hours.

Oxidation reaction of *o*-phenylenediamine

Three different types of PEO-coated CuPt nanorods were used as catalysts for the oxidation reaction of OPD in the presence of H$_2$O$_2$. 100 μl of 30% H$_2$O$_2$ and 50 μl of 0.02 M OPD were added to H$_2$O. Each type of CuPt aqueous solution (sphere, short rod, long rod) was added to the mixture. The amount of platinum in the solution was kept constant at 26.5 μM, and the total volume was maintained at 3 ml. The progress of the oxidation reaction was monitored at room temperature by recording UV-Vis absorption spectra at 2 min intervals using the scanning kinetics mode.

Results and discussions

Synthesis of CuPt nanorods with different aspect ratios

CuPt nanorods with different ARs were synthesized by tuning the ratio of OA to OLA. It is well-known that the AR of inorganic nanorods can be influenced by the choice of the capping agent that attracts specific atoms.[41] In this study, an increase in the OLA/OA ratio results in higher AR of nanorods.

For example, TEM image in Fig. 1(a) depicts CuPt nanorods synthesized with the OA/OLA ratio of 2 : 3. Histogram in Fig. 1(b) represents the statistical distribution of nanorod AR, which was obtained from image analysis of more than 700 nanorods.

However, even with very careful control of the OLA/OA ratio during synthesis, the as-synthesized product had a very broad distribution of nanorod AR, as shown in Fig. 1. In addition, a fraction of spherical particles was also present in the product, which required further purification. Two different steps were performed to obtain highly monodisperse nanorods. In the first step, the soluble/insoluble solvent mixing method, as-synthesized nanorods were dispersed in a 50 : 50 mixture of hexane and acetone and the desired product was separated by precipitation.[39] In the second step, complete purification of nanorods was achieved using the density-gradient method,[42] which utilizes the mass difference between short and long NRs. By adding nanorods to solvent layers of different densities, nanorods can be separated by aspect ratio. Accordingly, to purify our nanorods, we mixed DCM (ρ = 1.33 g ml^{-1}) and cyclohexane (ρ = 0.779 g ml^{-1}) to produce five layers with different densities. Because it is easier for the heavier CuPt NRs to pass through different density layers than the lighter spherical CuPt nanoparticles to do so, CuPt NRs were located in the bottom layer after the centrifugation at 20 000 rpm for 3 h, as shown in Fig. 2.
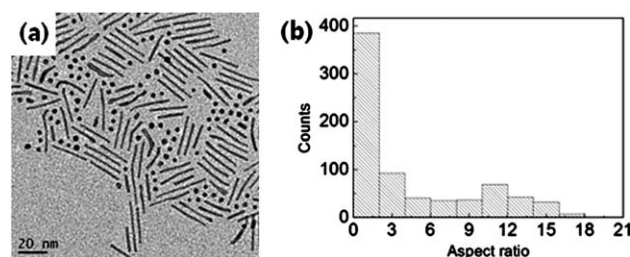
Fig. 1 (a) TEM image of CuPt nanorods synthesized with the volume ratio of OA to OLA = 2 : 3. (b) Histogram of the aspect ratio of as-synthesized CuPt nanorods. The statistics were obtained from image analysis of more than 700 particles.

Fig. 3 represents the TEM images of the purified CuPt nanorods with three different ARs ranging from 1 to 11. As evident from Fig. 3, nanorod purification was performed properly for all three nanorods. For convenience, the spherical CuPt (AR = 1.0), the short CuPt (AR = 5.6) and the long CuPt (AR = 11.1) nanoparticles are denoted as **CuPt-S**, **CuPt-SR** and **CuPt-LR**, respectively. It should be noted that while the long axis increases from 2.5, 14.0 to 27.4 nm for **CuPt-S**, **CuPt-SR** and **CuPt-LR**, respectively, the short axis for all nanorods remains constant at 2.5 nm. Therefore, our system is ideal for investigating the effect of AR on the properties of the nanorods.

Synthesis of PEO-SH and PEO coated CuPt nanorods

In this study, PEO-SH polymers were synthesized from hydroxyl-terminated PEO. A three-step reaction was performed to produce a well-defined thiol group at the end of the PEO chain. The molecular weight (M_n) of PEO chain was designed to be low in order to alleviate the steric hindrance effect and allow efficient ligand replacement by PEO-SH on the CuPt nanorods.

The completion of the reaction after each reaction step was confirmed by NMR analysis, as shown in Fig. 4. After the first step to form PEO-SO$_3$CH$_3$, the peak corresponding to the CH$_3$ protons appears at 3.1 ppm, while the peak for the –OH proton around 2.6 ppm disappears completely (Fig. 4(b)). In the second step, a new peak for PEO-SCOCH$_3$ appears at 2.4 ppm, while the peak for PEO-SO$_3$CH$_3$ disappears. Finally, a unique multiplet of peaks corresponding to the –SH protons is detected around 2.7 ppm. From these results, it was concluded that a complete exchange of the functional end-group had taken place.

The synthesized PEO-SH polymers were used in a ligand exchange of the CuPt nanorod surface. It is well-known that a thiol-terminated polymer can bind to the surface of various inorganic nanoparticles (*i.e.* Au, Ag, Pt, *etc.*) more strongly than
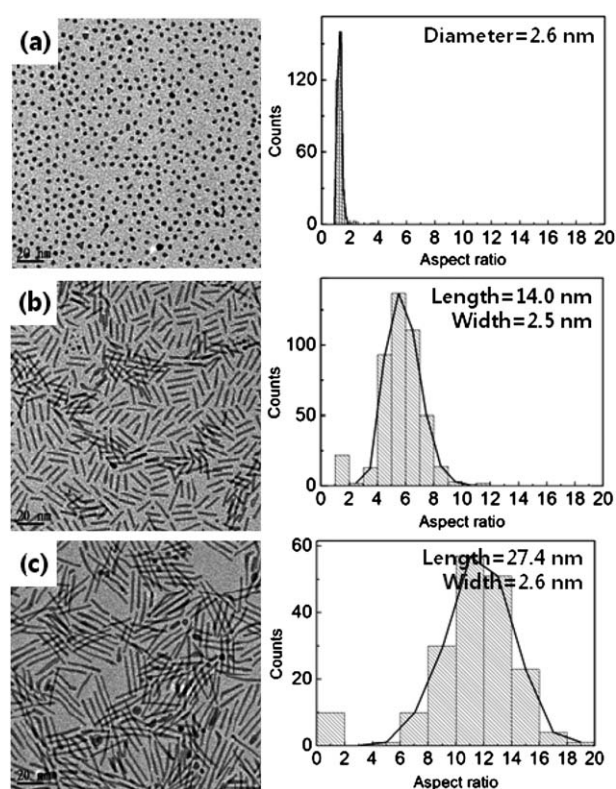

Fig. 3 TEM image of CuPt nanorods with three different ARs after purification. The AR of the nanorods was controlled by adding different ratios of OA to OLA in the synthesis. (a) Spherical CuPt nanoparticles (AR = 1.0) (**CuPt-S**). (b) Short CuPt nanorods (AR = 5.6 ± 1.6) (**CuPt-SR**). (c) Long CuPt nanorods (AR = 11.1 ± 3.3) (**CuPt-LR**). The scale bar is 20 nm. The plots on the right side represent the statistical distribution of the ARs obtained from corresponding TEM images.

polymers with other functional end groups.[43,44] As shown in Fig. 5, OA and OLA ligands were initially present on the CuPt nanorods. And the photograph image in Fig. 5(a) showed that OA and OLA-coated CuPt nanorods were well-dispersed in the nonpolar solvent of hexane. In contrast, after ligand exchange, CuPt nanorods were completely transferred to the water phase with good dispersion, which indicates that the ligand exchange by PEO-SH was performed successfully (Fig. 5(b)).
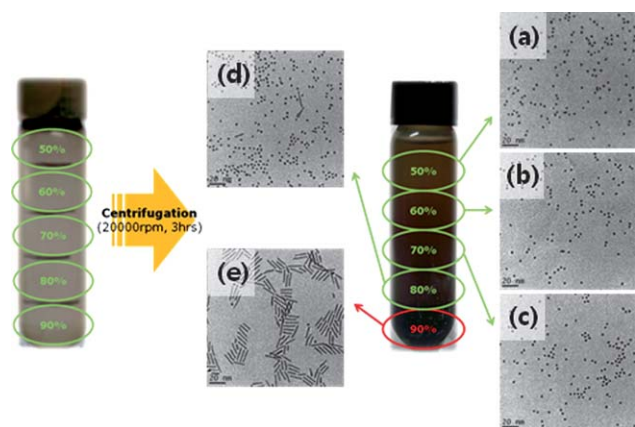
Fig. 2 The process of nanorod separation by the density gradient method. Digital image of ultracentrifuge vessel containing five layers of DCM and cyclohexane solutions with different volume ratios and densities. DCM : cyclohexane volume ratio: (a) 50 : 50 in layer (1.055 g ml^{-1}), (b) 60 : 40 in layer (1.110 g ml^{-1}), (c) 70 : 30 in layer (1.165 g ml^{-1}), (d) 80 : 20 in layer (1.224 g ml^{-1}) and (e) 90 : 10 in layer (1.275 g ml^{-1}). CuPt nanorods in toluene were added to the top of the first layer. After centrifugation at 20 000 rpm for 3 h, the bottom layer (e) in the tube contained purified CuPt nanorods. The inset TEM images represent the CuPt nanorods in each layer after separation.
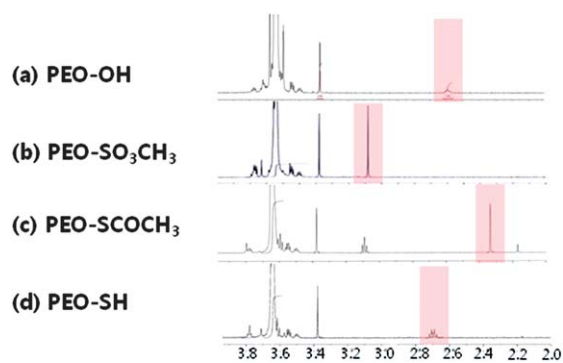
Fig. 4 ^{1}H-NMR data of (a) PEO-OH, (b) PEO-SO$_3$CH$_3$, (c) PEO-SCOCH$_3$ and (d) PEO-SH. PEO-SH was synthesized from PEO-OH *via* a three-step reaction.
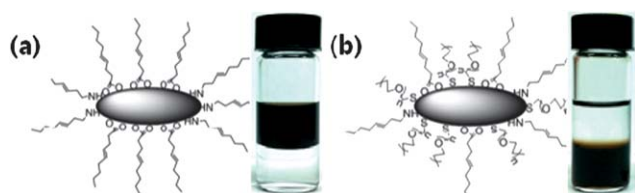
Fig. 5 Schematic diagrams of (a) OA/OLA-coated CuPt nanorods and (b) PEO-coated CuPt nanorods. As can be visualized in two different photographs, the OA/OLA coated CuPt nanorods are soluble in the hexane phase, whereas the PEO-coated CuPt nanorods are well-dispersed in the water phase.

Furthermore, the corresponding TEM images provide additional evidence of ligand exchange, demonstrating that PEO-coated CuPt nanorods including **CuPt-S** (AR = 1.0), **CuPt-SR** (AR = 5.6) and **CuPt-LR** (AR = 11.1) were well-dispersed in the water phase without aggregation (Fig. 6).

## Catalytic properties of CuPt nanorods in water

To examine the catalytic properties of CuPt nanorods in water, a peroxidase-like reaction of OPD oxidation was performed by using PEO-coated CuPt nanorods as catalysts. Pt alloy nanoparticles are known to catalyze the decomposition of superoxide free radicals and H_2O_2.[45] Since this type of enzyme-mimicking reaction occurs only in the aqueous phase, the phase transfer of shape-controlled nanoparticles into the water phase is a prerequisite for their application as catalysts. OPD is oxidized into a yellow solution of 2,3-diaminophenazine during the reaction; therefore, the progress of the OPD reaction can be monitored with UV-Vis absorbance spectroscopy by measuring the increase in peak intensity at 425 nm. In addition, to investigate the effect of AR on the catalytic activity, three different OPD reactions were performed using **CuPt-S**, **CuPt-SR** and **CuPt-LR**. The **CuPt-S** particles showed highest catalytic activity, and **CuPt-SR** and **CuPt-LR** nanorods had lower activities, as shown in Fig. 7.

To understand the difference in activity of CuPt nanorods with various ARs, the bulk and surface composition of CuPt nanorods was measured by inductively coupled plasma (ICP) and X-ray photoelectron spectroscopy (XPS), respectively. Table 1 shows that there is a difference between the bulk and surface composition of CuPt nanorods. Specifically, the Pt mole ratio appears to be larger at the surface than in the bulk, indicating that the surface of CuPt nanorods is rich in Pt.

Furthermore, the number of Pt atoms (N_{Pt}) at the surface and in the bulk was calculated based on the amount of platinum (0.0795 μg) used, the nanorod size, and the bulk and surface
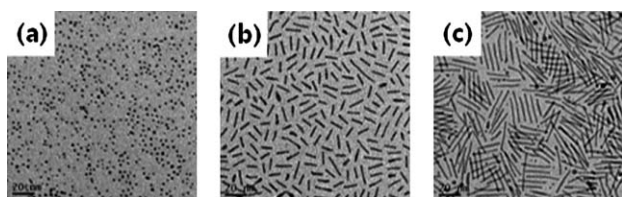
Fig. 6 TEM images of PEO-coated CuPt nanorods dispersed in water: (a) **CuPt-S**, (b) **CuPt-SR** and (c) **CuPt-LR**. The scale bar is 20 nm.
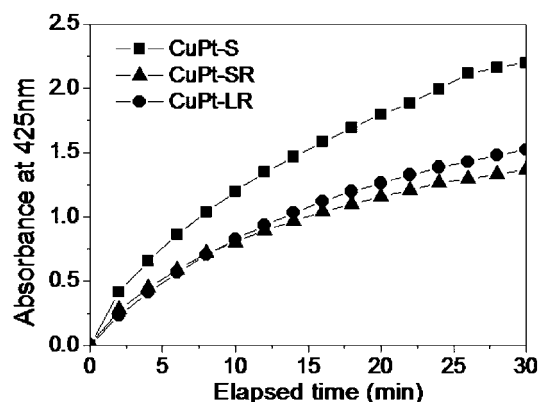
Fig. 7 OPD oxidation reaction using three different CuPt nanorods as catalyst was monitored by UV-Vis absorbance measurements at 425 nm as a function of reaction time (**CuPt-S** (squares), **CuPt-LR** (circles), **CuPt-SR** (triangles)).

Table 1 Characteristics of PEO-coated CuPt nanorods. The bulk composition in the nanorods was estimated by ICP measurements, while the surface composition was determined by XPS measurements. Comparison of Pt mole ratio between ICP and XPS results clearly shows that all nanorods have a Pt-rich surface

		Pt mole ratio in nanorods	
CuPt-PEO	Aspect ratio	ICP (bulk)	XPS (surface)
CuPt-S	1.0	0.512	0.667
CuPt-SR	5.6	0.485	0.630
CuPt-LR	11.1	0.464	0.645

compositions. The atomic composition on the very top surface was calculated from XPS data[46] although it should be noted that XPS is not a perfectly surface-sensitive technique. The number was determined to be 1.86×10^{14} for **CuPt-S**, 1.40×10^{14} for **CuPt-SR**, and 1.39×10^{14} for **CuPt-LR**, respectively. There is little difference in the number of surface Pt atoms for the short and long nanorods, but both have only 75% of the surface Pt atoms compared to spheres. Since Cu atoms in the CuPt nanorods do not have any reactivity in the OPD oxidation, this difference in surface Pt atoms between spheres and rods can be correlated to the difference in oxidation activity shown in Fig. 7. **CuPt-S** nanoparticles exhibited higher catalytic activity due to the presence of a higher number of surface Pt atoms. Efficient catalytic oxidation of OPD in the aqueous phase clearly demonstrates that CuPt nanorods are well-dispersed in the water phase, and the metal surface is accessible for catalytic surface reaction.

Conclusions

CuPt nanorods with various ARs were synthesized by thermal decomposition in the presence of nonpolar surface-stabilizing organic molecules (OA and OLA), and subsequently purified by the density-gradient method. The prepared **CuPt-S** with AR of 1.0, **CuPt-SR** with AR of 5.6, and **CuPt-LR** with AR of 11.1 exhibited high shape monodispersity and a short axis with the same length, making this system ideal for investigating the effect

This journal is © The Royal Society of Chemistry 2011

J. Mater. Chem., 2011, **21**, 11956–11960 | 11959

of AR on the properties of nanorod. Complete phase transfer was achieved by exchanging nonpolar surface-stabilizing organic molecules with a water-soluble PEO-SH polymer. In addition, water-soluble nanorods were investigated for their activity in a peroxidase-like reaction of OPD oxidation in water. The PEO-coated nanorods showed a high activity for OPD oxidation in the aqueous phase, indicating that the nanorods were well-dispersed in water, and their metal surfaces were available for surface reactions. The spheres with the greatest amount of surface Pt atoms showed the highest catalytic activity.

Acknowledgements

References

1 W. U. Huynh, J. J. Dittmer and A. P. Alivisatos, *Science*, 2002, **295**, 2425–2427.
2 D. L. Feldheim, K. C. Grabar, M. J. Natan and T. E. Mallouk, *J. Am. Chem. Soc.*, 1996, **118**, 7640–7641.
3 S. H. Sun, E. E. Fullerton, D. Weller and C. B. Murray, *IEEE Trans. Magn.*, 2001, **37**, 1239–1243.
4 C. J. Murphy, T. K. San, A. M. Gole, C. J. Orendorff, J. X. Gao, L. Gou, S. E. Hunyadi and T. Li, *J. Phys. Chem. B*, 2005, **109**, 13857–13870.
5 W. P. McConnell, J. P. Novak, L. C. Brousseau, R. R. Fuierer, R. C. Tenent and D. L. Feldheim, *J. Phys. Chem. B*, 2000, **104**, 8925–8930.
6 K. L. Kelly, E. Coronado, L. L. Zhao and G. C. Schatz, *J. Phys. Chem. B*, 2003, **107**, 668–677.
7 J. Bang, S. Lee, B. Lee, B. J. Kim, J. Park, M. Yoo, W. K. Bae, K. Char, C. J. Hawker and J. H. Cho, *J. Am. Chem. Soc.*, 2009, **131**, 2579–2587.
8 M. Yoo, S. Kim, J. Lim, E. J. Kramer, C. J. Hawker, B. J. Kim and J. Bang, *Macromolecules*, 2010, **43**, 3570–3575.
9 B. J. Kim, G. H. Fredrickson, J. Bang, C. J. Hawker and E. J. Kramer, *Macromolecules*, 2009, **42**, 6193–6201.
10 B. J. Kim, G. H. Fredrickson, C. J. Hawker and E. J. Kramer, *Langmuir*, 2007, **23**, 7804–7809.
11 R. Narayanan and M. A. El-Sayed, *J. Phys. Chem. B*, 2005, **109**, 12663–12676.
12 S. Eustis and M. A. El-Sayed, *Chem. Soc. Rev.*, 2006, **35**, 209–217.
13 C. Besson, E. E. Finney and R. G. Finke, *J. Am. Chem. Soc.*, 2005, **127**, 8179–8184.
14 N. Pradhan, A. Pal and T. Pal, *Colloids Surf., A*, 2002, **196**, 247–257.
15 A. R. Tao, S. Habas and P. D. Yang, *Small*, 2008, **4**, 310–325.
16 L. C. Courrol, F. R. D. O. Silva and L. Gomes, *Colloids Surf., A*, 2007, **305**, 54–57.
17 D. Guin, S. V. Manorama, J. N. L. Latha and S. Singh, *J. Phys. Chem. C*, 2007, **111**, 13393–13397.
18 Q. Fang, G. He, W. P. Cai, J. Y. Zhang and I. W. Boyd, *Appl. Surf. Sci.*, 2004, **226**, 7–11.
19 A. Henglein, *J. Phys. Chem. B*, 2000, **104**, 1206–1211.
20 W. Abidi, P. R. Selvakannan, Y. Guillet, I. Lampre, P. Beaunier, B. Pansu, B. Palpant and H. Remita, *J. Phys. Chem. C*, 2010, **114**, 14794–14803.
21 H. J. Hah, S. M. Koo and S. H. Lee, *J. Sol-Gel Sci. Technol.*, 2003, **26**, 467–471.
22 J. Chen, Y. Xiang, Y. Yin and Y. Xia, *Small*, 2006, **2**, 1340–1343.
23 X. W. Wu, C. Liu, L. Li, P. Jones, R. W. Chantrell and D. Weller, *J. Appl. Phys.*, 2004, **95**, 6810–6812.
24 S. H. Sun, H. Zeng, D. B. Robinson, S. Raoux, P. M. Rice, S. X. Wang and G. X. Li, *J. Am. Chem. Soc.*, 2004, **126**, 273–279.
25 Q. L. Zhang, S. Gupta, T. Emrick and T. P. Russell, *J. Am. Chem. Soc.*, 2006, **128**, 3898–3899.
26 S. B. Kim, C. Cai, S. Sun and D. A. Sweigart, *Angew. Chem., Int. Ed.*, 2009, **48**, 2907–2910.
27 M. Kim, Y. F. Chen, Y. C. Liu and X. G. Peng, *Adv. Mater.*, 2005, **17**, 1429–1432.
28 L. E. Pell, A. D. Schricker, F. V. Mikulec and B. A. Korgel, *Langmuir*, 2004, **20**, 6546–6548.
29 A. Dong, X. Ye, J. Chen, Y. Kang, T. Gordon, J. M. Kikkawa and C. B. Murray, *J. Am. Chem. Soc.*, 2010, **133**, 998–1006.
30 J. Xie, C. Xu, N. Kohler, Y. Hou and S. Sun, *Adv. Mater.*, 2007, **19**, 3163–3166.
31 J. W. Hotchkiss, A. B. Lowe and S. G. Boyes, *Chem. Mater.*, 2006, **19**, 6–13.
32 Y. G. Sun and Y. N. Xia, *Science*, 2002, **298**, 2176–2179.
33 B. Wiley, T. Herricks, Y. G. Sun and Y. N. Xia, *Nano Lett.*, 2004, **4**, 1733–1739.
34 Y. D. Yin, C. Erdonmez, S. Aloni and A. P. Alivisatos, *J. Am. Chem. Soc.*, 2006, **128**, 12671–12673.
35 J. B. He, P. Kanjanaboos, N. L. Frazer, A. Weis, X. M. Lin and H. M. Jaeger, *Small*, 2010, **6**, 1449–1456.
36 N. R. Jana and X. G. Peng, *J. Am. Chem. Soc.*, 2003, **125**, 14280–14281.
37 P. de la Presa, M. Multigner, J. de la Venta, M. A. Garcia and M. L. Ruiz-Gonzalez, *J. Appl. Phys.*, 2006, **100**, 123915.
38 X. C. Sun, C. J. Thode, J. K. Mabry, J. W. Harrell, D. E. Nikles, K. Sun and L. M. Wang, *J. Appl. Phys.*, 2005, **97**, 10Q901.
39 Q. S. Liu, Z. Yan, N. L. Henderson, J. C. Bauer, D. W. Goodman, J. D. Batteas and R. E. Schaak, *J. Am. Chem. Soc.*, 2009, **131**, 5720–5721.
40 A. K. Oyelere, P. C. Chen, X. H. Huang, I. H. El-Sayed and M. A. El-Sayed, *Bioconjugate Chem.*, 2007, **18**, 1490–1497.
41 Y. H. Wei, S. Chen, B. Kowalczyk, S. Huda, T. P. Gray and B. A. Grzybowski, *J. Phys. Chem. C*, 2010, **114**, 15612–15616.
42 L. Bai, X. J. Ma, J. F. Liu, X. M. Sun, D. Y. Zhao and D. G. Evans, *J. Am. Chem. Soc.*, 2010, **132**, 2333–2337.
43 S. F. Wuister, I. Swart, F. van Driel, S. G. Hickey and C. D. Donega, *Nano Lett.*, 2003, **3**, 503–507.
44 Y. Tanaka and S. Maenosono, *J. Magn. Magn. Mater.*, 2008, **320**, L121–L124.
45 W. W. He, X. C. Wu, J. B. Liu, X. N. Hu, K. Zhang, S. A. Hou, W. Y. Zhou and S. S. Xie, *Chem. Mater.*, 2010, **22**, 2988–2994.
46 J. Jasieniak and P. Mulvaney, *J. Am. Chem. Soc.*, 2007, **129**, 2841–2848.